

Vehicle System Dynamics: International Journal of Vehicle Mechanics and Mobility

Publication details, including instructions for authors and subscription information:

<http://www.tandfonline.com/loi/nvsd20>

An insight into linear quarter car model accuracy

Damien Maher^a & Paul Young^a

^a School of Mechanical Engineering, Dublin City University, Dublin 9, Ireland

Published online: 08 Sep 2010.

To cite this article: Damien Maher & Paul Young (2011): An insight into linear quarter car model accuracy, *Vehicle System Dynamics: International Journal of Vehicle Mechanics and Mobility*, 49:3, 463-480

To link to this article: <http://dx.doi.org/10.1080/00423111003631946>

PLEASE SCROLL DOWN FOR ARTICLE

Full terms and conditions of use: <http://www.tandfonline.com/page/terms-and-conditions>

This article may be used for research, teaching, and private study purposes. Any substantial or systematic reproduction, redistribution, reselling, loan, sub-licensing, systematic supply, or distribution in any form to anyone is expressly forbidden.

The publisher does not give any warranty express or implied or make any representation that the contents will be complete or accurate or up to date. The accuracy of any instructions, formulae, and drug doses should be independently verified with primary sources. The publisher shall not be liable for any loss, actions, claims, proceedings, demand, or costs or damages whatsoever or howsoever caused arising directly or indirectly in connection with or arising out of the use of this material.

An insight into linear quarter car model accuracy

Damien Maher* and Paul Young

School of Mechanical Engineering, Dublin City University, Dublin 9, Ireland

(Received 30 June 2009; final version received 17 January 2010)

The linear quarter car model is the most widely used suspension system model. A number of authors expressed doubts about the accuracy of the linear quarter car model in predicting the movement of a complex nonlinear suspension system. In this investigation, a quarter car rig, designed to mimic the popular MacPherson strut suspension system, is subject to narrowband excitation at a range of frequencies using a motor driven cam. Linear and nonlinear quarter car simulations of the rig are developed. Both isolated and operational testing techniques are used to characterise the individual suspension system components. Simulations carried out using the linear and nonlinear models are compared to measured data from the suspension test rig at selected excitation frequencies. Results show that the linear quarter car model provides a reasonable approximation of unsprung mass acceleration but significantly overpredicts sprung mass acceleration magnitude. The nonlinear simulation, featuring a trilinear shock absorber model and nonlinear tyre, produces results which are significantly more accurate than linear simulation results. The effect of tyre damping on the nonlinear model is also investigated for narrowband excitation. It is found to reduce the magnitude of unsprung mass acceleration peaks and contribute to an overall improvement in simulation accuracy.

Keywords: quarter car model; suspension systems; simulation

1. Introduction and background

A vehicle suspension system is designed to optimise the grip between the tyres and the road surface to ensure good handling. It is also designed to maximise the comfort of passenger by reducing the acceleration of the car body and hence the forces on passengers. In the design and development of suspension systems, simulation and experimental testing play an important role in achieving the optimal compromise between these conflicting design goals.

Simulation of a suspension system consists of the construction of a mathematical model of the system and, by examining the behaviour of the model under various conditions, determine how a real system would behave if and when it is built [1]. The solutions to these mathematical models can be found analytically or numerically. In literature, the analytical quarter car model is said to be the most widely used suspension system model [2–5]. With the current trend of using four independent suspension systems on a single vehicle, the linear quarter car model offers quite a reasonable representation of the actual suspension system [3,4,6].

*Corresponding author. Email: damien.maher3@mail.dcu.ie

1.1. Quarter car model

A diagram of the classic linear two degree of freedom quarter car model can be seen in Figure 1. The model consists of a sprung mass which represents the mass of quarter of the vehicle chassis and the unsprung mass which represents the mass of a single wheel, tyre, shock absorber and suspension knuckle. The sprung and unsprung masses are connected using linear spring and viscous damping elements to represent the stiffness and damping of the shock absorber. The tyre is modelled as a linear spring in parallel with a viscous damper (point contact tyre model). Despite its simplicity, the linear quarter car model is very popular in the literature of suspension research. It has the following advantages over more complex models [7]:

- relationship between design and performance are easily understood;
- few design parameters;
- few performance parameters;
- single input system, leading to ease of computation of performance and
- ease of application of control theory to derive control laws.

It does not, however, give any representation of the geometrical effects of having four wheels and offers no possibility of studying the excitation of vehicle body roll and pitch motions. Two lesser used analytical models, the four degree of freedom half car model and seven degree of freedom full car model, are used when these parameters are of interest [8–10].

1.2. Quarter car model accuracy

Conflicting views are found in the literature on the accuracy of the linear quarter car model. Despite its widespread use, little dedicated research was found on the validity of the relatively simple model in predicting the movement of complex suspension systems.

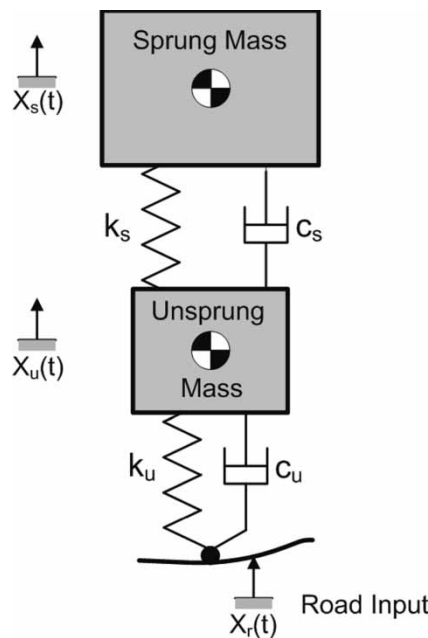


Figure 1. Two-DOF quarter car model.

A number of authors have cast doubts over the effectiveness of the linear quarter car model in predicting suspension movement in certain circumstances. Kim and Ro [3] wrote that the two mass quarter car model is effective in predicting the two dominant modes, sprung mass bouncing and wheel hopping. They did, however, have some reservations about the component data used in such simulations. The authors constructed a complex multibody model and used it to produce a two degree of freedom reduced order model. They estimated the component parameters for the reduced order model and found them to be very far from the measured component data. They also referred to work carried out by Kim *et al.* [4], in which it was shown that suspension kinematic structure has an influence on the effectiveness of the simple linear quarter car model. Türkay and Akçay [11] used a linear quarter car model to study the response of a vehicle to random road inputs. Their results showed how imprecise knowledge of the excitation road spectra would impact subsequent active suspension design. They recognised that the linear quarter car model is ‘too simple for performing a comprehensive analysis of the ride motion of the vehicle’ but also noted that significant insight into the problem can be obtained using this simple model. Etman *et al.* [12] compared the optimum parameters of a stroke dependent truck damper for both a linear quarter car model of the front side of a truck and a 34 degree of freedom multibody full truck model. It was concluded that the step form the quarter car model to the full scale model was ‘pretty large’, due to the fact that a great deal of the dynamic behaviour of the truck was not included in the quarter car model. They did, however, note that a reasonable resemblance of the global response behaviour was present between the two models.

A popular view among authors is that the linear quarter car model is used due to its simplicity and that the qualitative information it provides in the initial stages of design outweighs the inaccuracy [7,13,14]. Elmadany and Abduljabbar stated that it captures the most basic features of the real vehicle problem. They followed this by saying that when a detailed model of vehicle motion is required, more elaborate models (two or three dimensional models) must be used which take account of features omitted from the quarter car model [15]. An important property of the quarter car model is that it properly represents the problem of controlling wheel load variations and contains suspension system forces which are properly applied between unsprung and sprung masses [7]. This fact has given rise to the widespread use of quarter car models in the development of active and semi-active suspension control strategies.

1.3. Tyre modelling

The pneumatic tyre serves an important purpose in suspension systems with respect to the isolation of road-induced vibration. There are a variety of tyre models in the literature with different levels of complexity. Tyre model complexity is determined by the frequency range of interest of the study [16].

In the low-to-intermediate frequency range, the most widely used and simple tyre model is the point contact model [17,18]. It consists of a linear spring in parallel with a linear viscous damper. This is considered to give a relatively good approximation of tyre forces generated when a tyre is in contact with small amplitude, long wavelength road profiles. The enveloping behaviour of tyres as they roll over small obstacles cannot be accounted for in such a model as it does not consider the tyre geometry and elasticity in the contact zone. More complex tyre models are required for noise, vibration and harshness investigations [16,18].

Conflicting views were also found on the issue of tyre damping in quarter car models. The view that tyre damping is typically small, and is therefore insignificant compared with shock absorber damping is shared by a number of authors [10,19–21]. The placement of tyre damping in the quarter car model has also been given as a reason to neglect its effects [7].

It was noted in [22] that tyre damping is often neglected in suspension simulations due to the fact that it is difficult to estimate.

On the other hand, some authors argue that the role of tyre damping in vehicle dynamics is overshadowed by factors which are presumed to be more important [23,24]. It is often neglected even in view of the fact that the tyre damping ratio is generally accepted to be between 0.03 and 0.10, depending on tyre size and type [25]. Levitt and Zorka [23] published a paper on the influence of tyre damping in quarter car active suspension models. The authors urged that considerable care be taken in setting tyre damping to zero when developing quarter car models for control applications. Nonzero tyre damping was shown to couple the motions of the sprung and unsprung masses at all frequencies and lead to substantially different transfer functions for root mean square (RMS) body acceleration. Türkay and Akçay studied the effect of tyre damping on the performance limitations of quarter car active suspension models subject to random road excitation. Results showed that tyre damping can have a significant influence on the closed loop performance of the active suspension system [25].

1.4. Shock absorber modelling

The shock absorber is one of the most important elements in a vehicle suspension system, it is also one of the most nonlinear and complex elements to model. Duym [26] highlighted that attempts in the past to simulate vehicle behaviour showed poor correlation with measured values due to the fact that shock absorbers were modelled as pure linear elements. Duym also stated that the linear modelling of shock absorbers has been rejected and replaced by two-slope or three-slope models which better represent the most important nonlinearity in the characteristic diagram.

The helical spring component of the shock absorber is often treated as a simple massless element in dynamic analysis. It was noted in [27] that this assumption is valid at low frequencies. At higher frequencies, the dynamic stiffness is found to increase sharply due to internal resonance in the spring. For coil springs typically used in automotive applications, this was found to happen at frequencies around 40 Hz [27].

1.5. Quarter car experimental testing

Suspension experimental testing provides a method of tuning and testing suspension setups for specific applications. Quarter car test rigs are designed to provide realistic suspension movement while eliminating the need to have a full vehicle present for testing purposes. Gobbi *et al.* [28] noted that very few applications are presented in the literature referring to full suspension indoor testing. Many of the quarter car test setups found in literature fall into one of three categories.

The first category simplifies the movement of the sprung and unsprung masses by constraining their motion in the vertical direction. An example of this type of rig can be found in [29]. This type of rig is primarily used for active and semi-active control system development and validation [30,31].

The second type of quarter car rig provides a more realistic suspension setup by using a full suspension system, including wheel and tyre. Langdon designed a rig of this type [32], which was used in research by Ziegenmeyer [33] to estimate the disturbance inputs to the tyre. Excitation is provided by a hydraulic shaker system under the tyre, while allowing for the use of an actual suspension system.

The third category of test rig is a rolling road type quarter car rig as used by Giorgetta *et al.* [34] and Gobbi *et al.* [28,35,36]. This type of rig consists of a drum which provides

a running contact surface for vehicle wheels. The suspension arm and shock absorber are attached to a sled system which is free to move in the vertical direction. Excitation is provided by cleats on the drum surface.

1.6. Paper outline

There is clearly a grey area surrounding the linear quarter car model in terms of when it can be used and for what types of simulation it can be used. This work examines both linear and nonlinear quarter car models with passive damping subject to sinusoidal excitation. Experimental testing and analysis of the major components of a quarter car test rig provides the parameters for these models. Simulations carried out using these models are compared with measured data from the suspension test rig at selected frequencies. Having first assessed the performance of the linear quarter car model, the performance improvements which can be obtained by including nonlinear components in the two mass quarter car model are quantified. The effect of tyre damping on the nonlinear simulation accuracy is also examined.

2. Measurement and simulation setup

2.1. Experimental testing setup

Figure 2 shows the laboratory test rig(quarter car rig) purpose-built for this research. The rig is a rolling road type rig with passive shock absorber and is designed to mimic a MacPherson Strut type car suspension system. The MacPherson strut system is popular among car manufacturers due to its relatively low cost and compact size. The suspension system consists of a wheel mounted on a stub axle which is connected to the suspension knuckle. The knuckle is attached to a frame representing the vehicle chassis using two parallel links. The shock absorber, an air damper unit with coil over spring, connects the suspension knuckle to the sprung mass. The

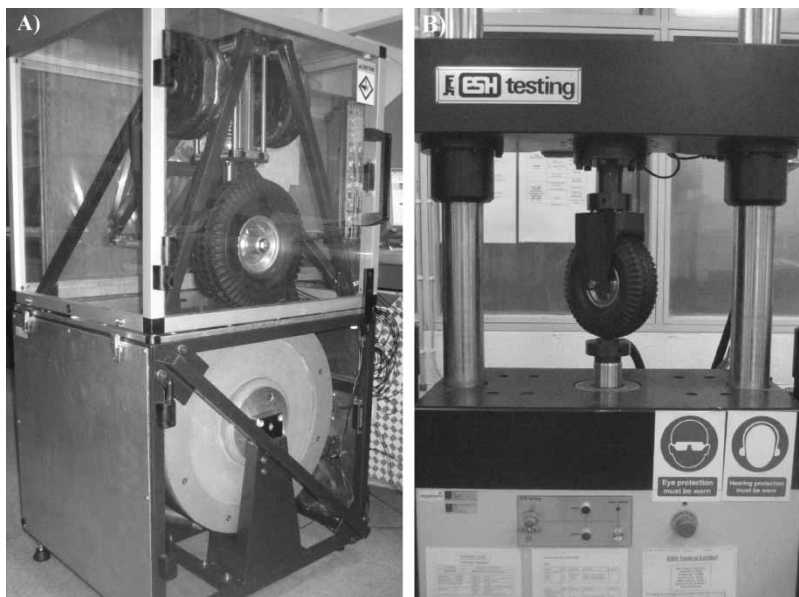


Figure 2. (a) Experimental test suspension rig and (b) ESH machine showing tyre test setup.

suspension system support structure consists of a truss system which supports parallel linear guides. The sprung mass is constrained to one degree of freedom (vertical) using this guide system, in a manner similar to other rigs in literature [28,29,32]. The rig support structure was tested to ensure that no resonant frequencies lie in the frequency range of interest of this study (1.6–24 Hz). The rig design allows for flexibility in the suspension setup. The sprung mass can be adjusted and the rig has interchangeable steel and rubber bushings at the chassis connection points. This allows the flexure of bushing to be included in, or excluded from, experimental tests. A variable speed motor drives computer numerical controlled (CNC) machined cams which provided the input to the system. The rig is computer-controlled through a MatlabTM-based simulation and analysis tool. This tool facilitates rapid side-by-side comparison of simulated and experimental results.

An ESHTM servo-hydraulic testing machine is used to perform isolated testing on individual suspension components. A picture of the ESHTM machine is shown in Figure 2. Experimental measurements on the quarter car rig and ESHTM machine are carried out using Brüel & Kjær'sTM PulseTM hardware/software system.

2.2. Simulation

The governing differential equations of motion of the linear quarter car model shown in Figure 1 are

$$m_u \ddot{x}_u + c_s(\dot{x}_u - \dot{x}_s) - c_u(\dot{x}_r - \dot{x}_u) + k_s(x_u - x_s) - k_u(x_r - x_u) = 0 \quad (1)$$

$$m_s \ddot{x}_s - c_s(\dot{x}_u - \dot{x}_s) - k_s(x_u - x_s) = 0 \quad (2)$$

where m_s represents the sprung mass and m_u the unsprung mass. k_u , c_u , k_s and c_s represents the tyre stiffness, tyre damping, spring stiffness and damper damping, respectively. x_u , x_s and x_r are the displacements of the unsprung mass, sprung mass and road input, respectively. Simulations are conducted in MatlabTM and SimulinkTM.

3. Suspension component characterisation

3.1. Tyre

Figure 2 shows the tyre isolated test setup. The test setup is based on the setup used by Burke and Olatunbosun to validate a finite element tyre model [37]. The tyre is tested both statically and dynamically at four different inflation pressures between 1.1 and 2.0 bar. During static testing the tyre shows an approximately linear force – displacement relationship in the 0–0.015 m range. For dynamic tests, a preload of 326 N is applied to the tyre. This is the load experienced by the tyre when mounted in the quarter car rig at rest. The tyre is excited using sinusoidal excitation. It is excited at frequencies between 0.5 and 14 Hz over an amplitude range of 0.0005 to 0.004 m. Under dynamic excitation, the tyre shows a slight hardening/softening spring characteristic at all frequencies and amplitudes. Hysteresis loops are also observed in the work diagrams. The energy loss per cycle due to internal friction is found to be independent of frequency, indicating the presence of hysteretic damping in the tyre.

Further analysis reveals that tyre stiffness increases with excitation frequency and decreases with excitation amplitude. The hardening/softening effect increases with excitation amplitude, while damping decreases with excitation amplitude. Two tyre models are developed, a linear tyre model and a nonlinear tyre model. The linear tyre model provides a good approximation of the tyre behaviour especially at higher inflation pressures where tyre deformation is less. The

nonlinear model takes into account the hardening/softening spring characteristic, frequency and amplitude dependence of tyre stiffness and also the tyre hysteretic damping.

The linear tyre model consists of a linear spring element. The stiffness is found experimentally to be 89,020 N/m. The nonlinear tyre model is shown in Figure 3. This tyre model has the same structure as the linear point contact model but is modified to include the effects of nonlinearities identified during isolated tyre testing. It consists of a nonlinear spring in parallel with a hysteretic damping element. The input signal to the tyre is smoothed using a moving average filter to represent the tyre enveloping and mechanical filter properties [38,39]. The tyre behaviour is governed by

$$F_{nt} = F_s + F_d \quad (3)$$

where F_{nt} is the nonlinear tyre force. F_s and F_d , the nonlinear spring force and the hysteretic damping force, respectively, are given by

$$F_s(x) = k_n(x + \alpha x^2) \quad (4)$$

$$F_d = c_{eq}\dot{x} \quad (5)$$

$$= \frac{\beta k_n}{2\pi f_e} \dot{x} \quad (6)$$

where k_n is the tyre stiffness, and is a function of excitation amplitude and frequency (f_e), while α is the magnitude of the stiffness squared term, and is also a function of excitation amplitude. β is the hysteretic damping coefficient and c_{eq} is the equivalent viscous damping coefficient.

3.2. Shock absorber

Characterisation of shock absorbers is usually carried out experimentally using mechanical test stands [40] and harmonic excitation [41,42]. In this work, the shock absorber (spring and damper combination) is tested both in isolation, using the ESH™ machine, and under operational conditions, mounted in the quarter car rig. The isolated shock absorber test setup is based on the methods used by Centro Ricerche FIAT (CRF) of Torino, Italy as presented in a case study by Worden and Tomlinson [43].

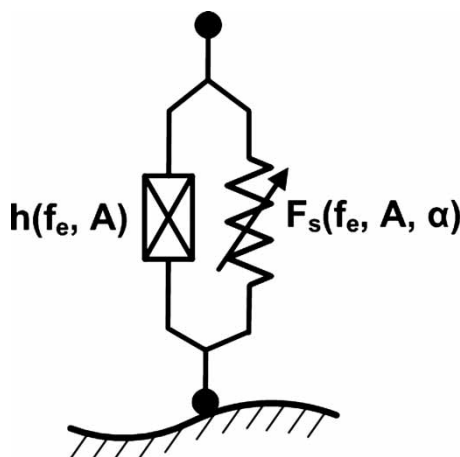


Figure 3. Nonlinear point contact tyre model.

A novel force measurement system is used which allows the measurement of shock absorber force during isolated and operational testing using the same force transducer setup. The force measurement setup uses a Kistler™ 9021A load washer and is calibrated using a Brüel & Kjær™ Type 8200 force sensor. Figure 4 shows the 9021A load washer mounted on top of the shock absorber piston during isolated testing with the Type 8200 force sensor mounted at the base of the shock absorber. Figure 4 also shows the 9021A load washer mounted on the quarter car rig, using the same mounting method. Although the isolated testing provides accurate results, the operational measurements provide a more useful shock absorber characteristic as it includes effects related to the shock absorber mounting.

During operational testing, the quarter car rig is set up with a cam which provides an approximately sinusoidal input with amplitude of 0.0005 m. The rig is run at individual frequencies, while measuring the sprung and unsprung mass accelerations along with shock absorber force. Brüel & Kjær™ Type 4508 accelerometers are used for acceleration measurement. The relative velocity and displacement across the damper are calculated from the acceleration measurements and are plotted against the shock absorber force to get the shock absorber characteristic (force – velocity) and work diagrams (force – displacement). To verify the results, the test is repeated with the sprung mass locked in its equilibrium position. This simplifies the suspension movement and eliminates inertia effects of the sprung mass from the force measurements. Essentially, this setup mimics the setup on the ESH™ hydraulic testing machine during isolated testing. The results closely matched those taken during full operational tests. Figure 5 shows two shock absorber characteristics obtained from operational testing at 7 and 10 Hz.

Based on these results, a generalised three slope shock absorber model is developed. The three slope model represents the major nonlinearity in the system, which is found from isolated testing to be static friction at low piston velocities. Outside the static friction zone, viscous damping is found to be the dominant damping mechanism. The equations representing the piecewise characteristic are [40]

$$f_d(\dot{z}) = \begin{cases} c_2(\dot{z} - c_5) + c_1c_5 & \text{for } \dot{z} > c_5, \\ c_1\dot{z} & \text{for } c_4 \leq \dot{z} \leq c_5, \\ c_3(\dot{z} - c_4) + c_1c_4 & \text{for } \dot{z} < c_4 \end{cases} \quad (7)$$

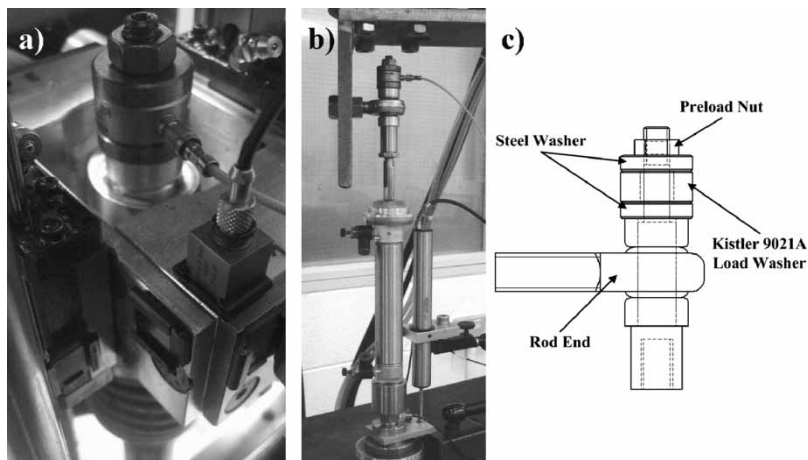


Figure 4. (a) Operational force measurement setup, (b) Isolated force measurement setup and (c) Force measurement schematic.

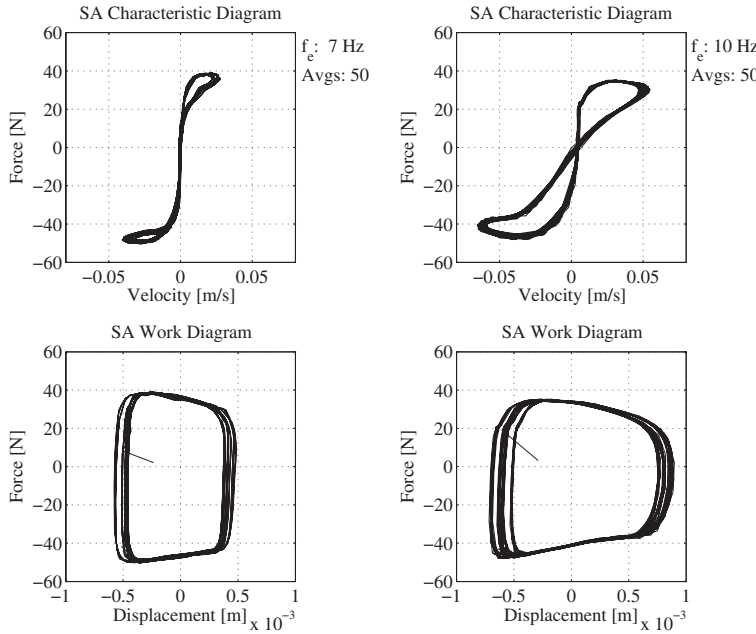


Figure 5. Shock absorber characteristic from operational test.

where f_d is the damper force, \dot{z} is damper piston velocity and the parameters c_1, c_2, c_3, c_4, c_5 to be identified are shown in Figure 6. For the linear simulations, a linear damper model is also fitted to the shock absorber characteristic.

The spring is also tested in isolation. The experimental test setup is the same as the tyre dynamic test. The spring stiffness does not show significant dependence on excitation frequency or amplitude. The mean dynamic spring stiffness is found to be 5.69 N/mm. The energy dissipation of the spring is negligible when compared with that of the damper.

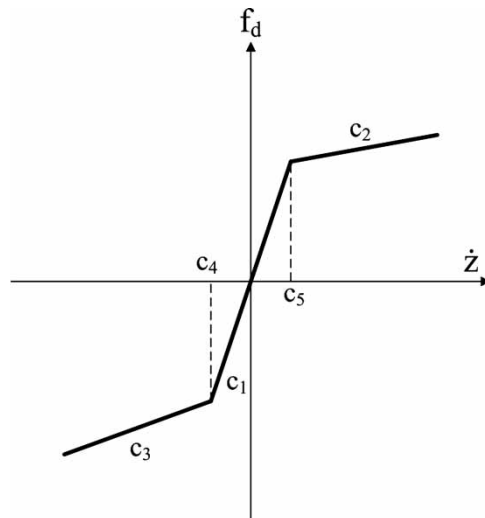


Figure 6. Damper Piecewise linear function (adapted from [34]).

4. Quarter car simulation

The quarter car rig is excited with an approximately sinusoidal excitation with peak-to-peak amplitude of 0.001 m in the 1.6 – 24.0 Hz frequency range. Fifty-six individual frequencies are used in this frequency range with a Δf value of 0.4 Hz. Tests are carried out at each frequency for 64 s and then averaged. The frequency spectrum of each averaged time history is calculated. The real and imaginary values are noted at the excitation frequency and are combined to give a response spectrum of the rig across the frequency range. At each measurement point, a linear model is fitted to the operational shock absorber characteristic. This technique of fitting the linear shock absorber model at each individual measurement frequency is required due to the nonlinear nature of the shock absorber. No single linear model will accurately represent the shock absorber across its full operational frequency range. Fitting a model at each measurement frequency ensures that the linear shock absorber model offers the best representation of the shock absorber characteristic at that individual frequency. Orthogonal linear regression is used to fit the linear shock absorber models to the measured data. The linear quarter car parameters fixed for the duration of this testing are shown in Table 1.

4.1. Linear quarter car simulation

The simulated linear quarter car spectra and measured quarter car spectra are shown in Figure 7. The linear quarter car simulation provides a reasonable approximation of the magnitude of the

Table 1. Linear quarter car parameters.

Parameter	Measured Value	Unit
m_u	8.0	kg
m_s	25.2	kg
k_s	5690	N/m
k_u	89,020	N/m

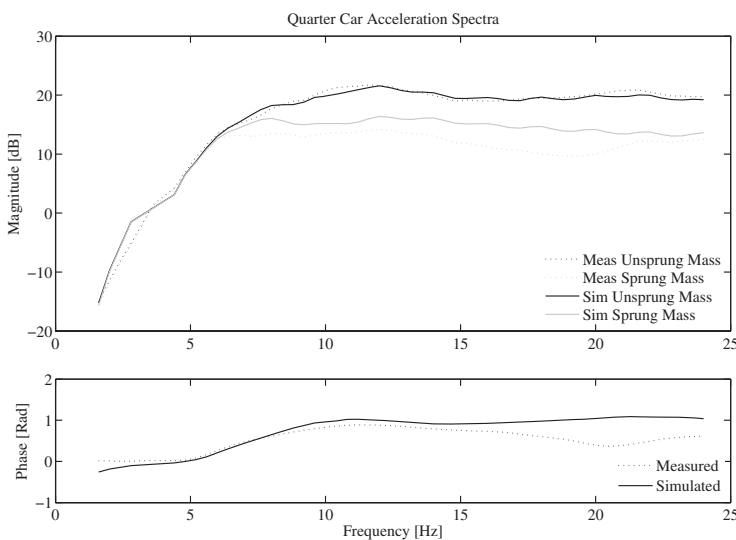


Figure 7. Linear quarter car model spectra between 1.6 and 24 Hz

unsprung mass acceleration across the full frequency range of the test. It does, however, over predict the magnitude of the sprung mass acceleration above 5 Hz. Further insight is gained by looking at individual frequencies. Figure 8 shows simulated and measured acceleration time history comparisons at 5.2 and 12.0 Hz. The RMS signal amplitudes are also shown. The simulation accurately predicts both unsprung and sprung mass acceleration amplitudes at 5.2 Hz. The percentage errors in acceleration RMS are 3.7% and 1.3% for the unsprung mass and sprung mass, respectively. At 12.0 Hz, the simulation underpredicts the unsprung acceleration and overpredicts the sprung mass acceleration. The percentage error is 19.1% for the unsprung mass and 30.9% for the sprung mass.

The presence of static friction in the damper is confirmed from the measured sprung and unsprung mass spectra. Notice how the measured sprung and unsprung mass spectra are almost identical below approximately 5 Hz. Correlation coefficients are calculated between the measured unsprung and sprung mass accelerations in the 1.6 – 24.0 Hz frequency range. The correlation coefficient is a measure of the strength of the relationship between the two signals. It is calculated using [44]

$$\rho_{xy}(\tau) = \frac{R_{xy}(\tau) - \mu_x \mu_y}{\sqrt{[R_{xx}(0) - \mu_x^2][R_{yy}(0) - \mu_y^2]}} \quad (8)$$

where $R_{xy}(\tau)$ is the cross-correlation between x and y at time τ , $R_{xx}(0)$ is the auto-correlation of x at $\tau = 0$, $R_{yy}(0)$ is the auto-correlation of y at $\tau = 0$, μ_x is the mean value of x and μ_y is the mean value of y . Correlation coefficients are calculated at $\tau = 0$. Correlation coefficients for measured accelerations are above 0.99 for excitation frequencies below approximately 5.0 Hz. This indicates that the unsprung and sprung mass movements are highly coupled below this frequency. The correlation coefficients at 5.2 and 12.0 Hz are 0.98 and 0.51, respectively.

This provides an insight into why the linear model is more accurate at 5.2 Hz than at 12.0 Hz. The measurement at 5.2 Hz is very close to the static friction zone and as a result the dominant mode of damping in the shock absorber at this frequency is due to friction

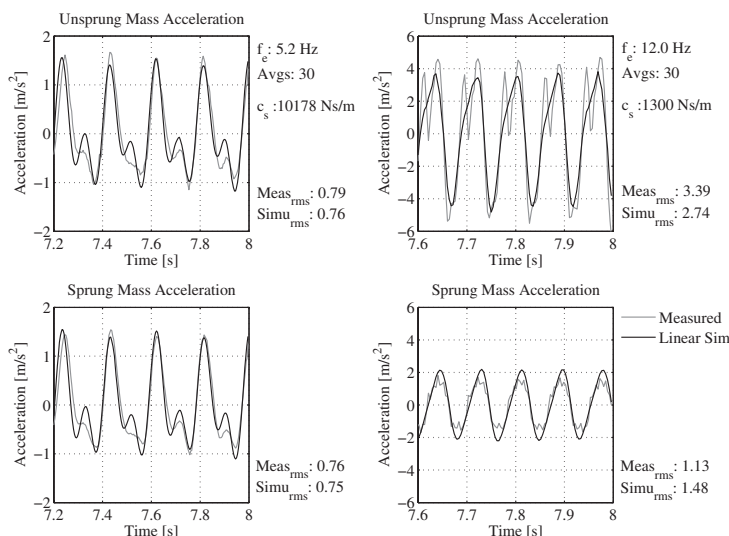


Figure 8. Linear quarter car simulation and measured data time history comparison.

damping. A linear damping model gives a reasonable approximation of this damping at 5.2 Hz due to the small relative velocity across the shock absorber. At 12.0 Hz, the damping is a combination of both friction damping and viscous damping due to the larger relative velocity and displacement across the shock absorber. A linear damping approximation at this frequency does not accurately describe the shock absorber characteristic. The effect of this static friction can be seen in the calculated linear damper coefficients. At 5.2 Hz the linear damping coefficient is 10,178 Ns/m compared with a value of 1300 Ns/m at 12.0 Hz.

4.2. Nonlinear quarter car simulation

A nonlinear quarter car model is developed and tested at selected frequencies. The goal of this particular analysis is to quantify the accuracy improvement which may be obtained with the inclusion of nonlinear suspension component models in a quarter car simulation.

The nonlinear quarter car model uses the nonlinear tyre model developed during isolated testing and also a trilinear damper model developed from operational testing. The frequencies selected for this test are 6.8 and 11.2 Hz. The optimised trilinear shock absorber model and equivalent linear shock absorber model for each of these frequencies are shown in Figure 9. The trilinear models are optimised using direct search methods. The optimisation is carried out in Matlab™ using the *patternsearch* function. The shock absorber model error is evaluated by calculating the normalised mean squared error (NMSE) between measured shock absorber force and the simulated shock absorber force for one cam cycle. The NMSE is calculated using

$$\text{NMSE}(\hat{x}) = \frac{1}{n\sigma_x^2} \sum_{i=1}^n (x_i - \hat{x}_i)^2 \quad (9)$$

where x is the measured data, \hat{x} is the simulation data and n is the number of samples. The trilinear shock absorber models give significantly smaller error magnitudes than their linear equivalents.

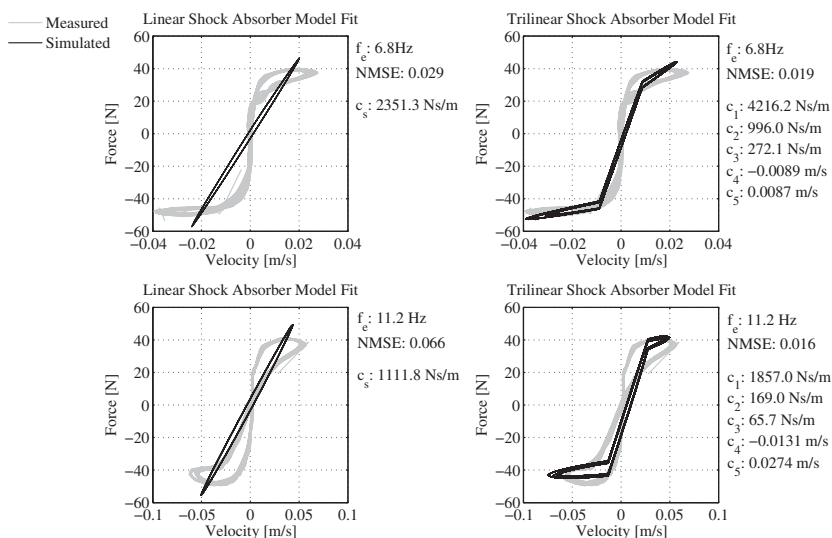


Figure 9. Linear and trilinear shock absorber models at 6.8 and 11.2 Hz.

4.2.1. Linear versus nonlinear quarter car simulation

The nonlinear simulation results are shown side by side with linear simulation results in Figures 10 and 11. The excitation frequency, damper parameters, measured acceleration RMS and simulated acceleration RMS values are plotted with each figure. In general, the results show that the nonlinear simulation provides a significant improvement over the linear simulation when compared with measured results from the quarter car rig. The nonlinear simulation accurately predicts both the unsprung and sprung mass accelerations in terms of magnitude and signal peak pattern. The linear simulation gives a reasonable approximation of the

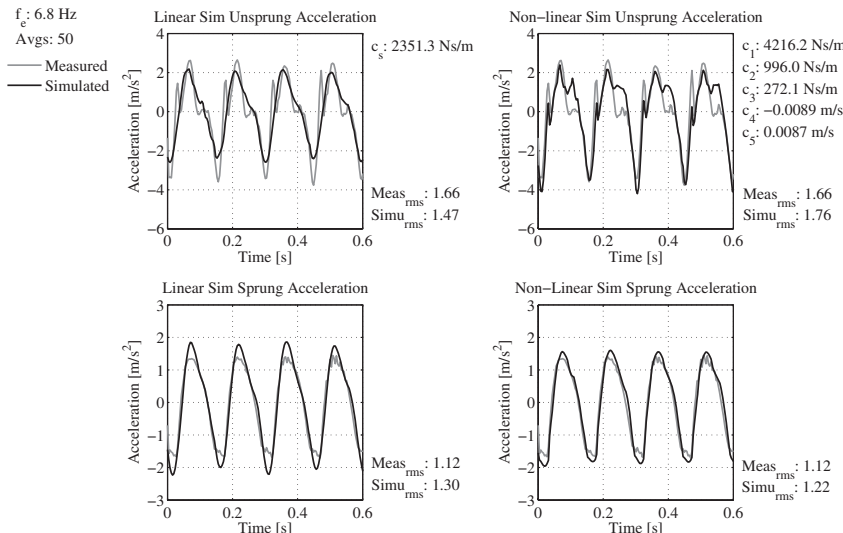


Figure 10. Linear and nonlinear quarter car simulation evaluation at 6.8 Hz.

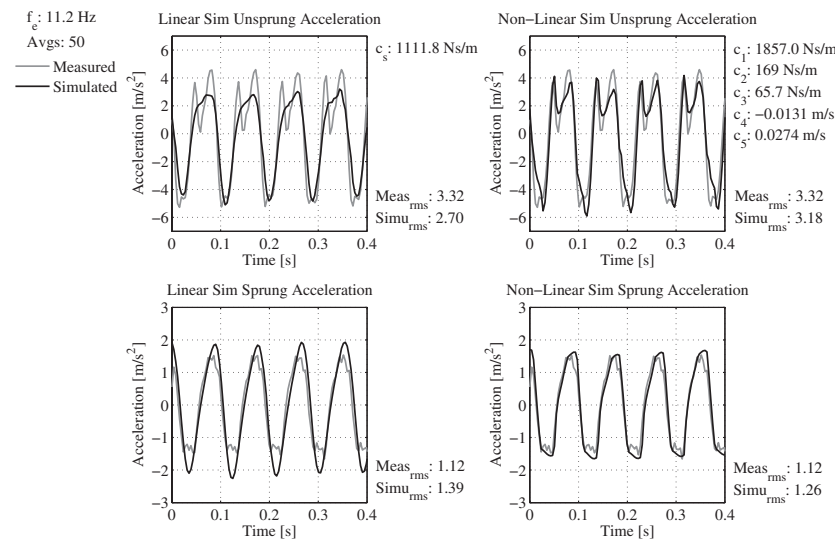


Figure 11. Linear and nonlinear quarter car simulation evaluation at 11.2 Hz.

magnitude of the unsprung mass acceleration but over predicts the magnitude of the sprung mass acceleration. It also gives a poor estimate of the signal peak pattern. At 6.8 Hz the linear simulation shows a 11.4% error in the unsprung mass acceleration and a 16.1% error in the sprung mass acceleration. The nonlinear simulation shows errors of 6.0% and 8.9% for the unsprung and sprung mass accelerations, respectively. At 11.2 Hz, the linear simulation shows an 18.7% error in the unsprung mass acceleration and a 24.1% error in the sprung mass acceleration. This is compared with 4.2% and 12.5% for the nonlinear simulation unsprung and sprung mass accelerations, respectively.

4.2.2. Effect of tyre damping

The introduction highlights differences of opinion among authors with regard to the importance of tyre damping in quarter car simulations. The damping of the tyre in this experimental investigation is quantified using isolated tyre testing. To test the effect that tyre damping has on simulation results, two quarter car simulations with optimised trilinear damper are run. Two tyre models are used, the first simulation uses a linear spring point contact model with no damping and the second a linear spring and viscous damper point contact model. The test is conducted at 10.4 Hz and the equivalent tyre viscous damping coefficient, c_u , is found using Equation (6) to be 138 Ns/m ($\zeta = 0.082$) at this frequency. The results from the two simulations are compared with measured results in Figure 12.

The simulation with tyre damping shows more damping in the peaks of the unsprung mass acceleration when compared with the simulation with no tyre damping. The simulation with no tyre damping and the simulation with tyre damping show maximum peak amplitudes of 6.4 and 4.3 m/s², respectively. This is compared with a measured maximum peak amplitude of 4.0 m/s². Both simulations show a percentage error of 4.7% in the RMS amplitude of the unsprung mass acceleration. The simulation with no tyre damping shows a percentage error of 17.8% for sprung mass acceleration RMS amplitude while the simulation with tyre damping reduces this error to 10.7%.

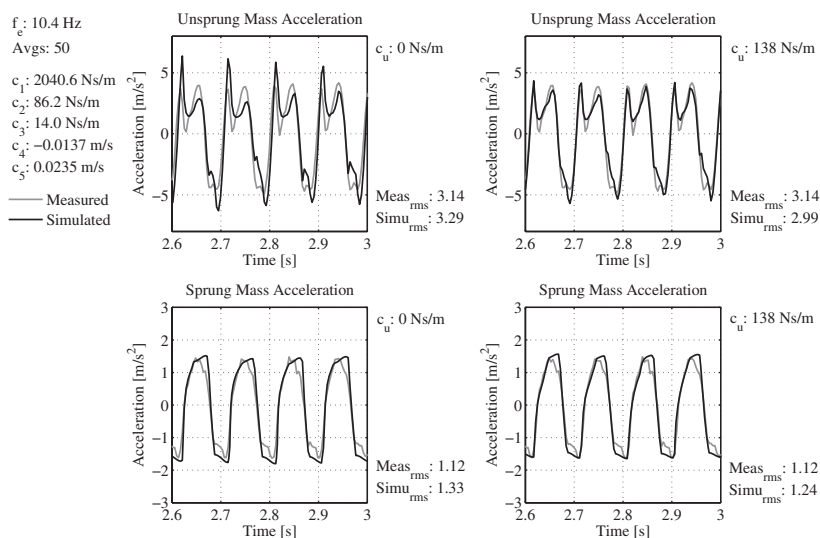


Figure 12. Tyre damping comparison at 10.4 Hz.

5. Discussion

Isolated component testing shows the shock absorber to be highly nonlinear. Static friction, asymmetry and hysteresis are observed. The static friction is found to be the most significant nonlinearity in the shock absorber. The nonlinearities identified in the shock absorber are consistent with those found in experimental investigations by other authors [40,41,45,46]. The tyre also shows hysteretic damping and a hardening/softening spring characteristic, but the magnitudes of the nonlinearities are small in comparison to the shock absorber.

Linear quarter car simulations are first examined. The quarter car rig is excited at fifty six individual frequencies, in the 1.6–24.0 Hz frequency range, using an approximately sinusoidal excitation. Viscous damping models are fitted to the shock absorber characteristic at each measurement frequency. This technique allows for optimal linear damper models to be used in the linear simulations at each excitation frequency. Due to the static friction nonlinearity, the optimal viscous damping coefficients at low shock absorber velocities are extremely high. The linear simulation is quite accurate in this low velocity static friction zone where the static friction nonlinearity dominates. The simulation accuracy may be aided by the fact that the relative motion between the unsprung and sprung masses is very small and as a result the shock absorber is effectively inactive at these low excitation velocities. As the excitation frequency increased, the relative motion across the shock absorber increased and the shock absorber model became more significant in terms of simulation accuracy. Outside the static friction zone, the linear simulations are found to give a reasonable approximation of the unsprung mass acceleration but overestimate the sprung mass accelerations. Figure 9 provides an insight into the reason behind sprung mass acceleration overestimation. Note how the optimal linear model significantly overestimates shock absorber force at higher excitation velocities. Overestimation of the shock absorber force would subsequently cause overestimation of the sprung mass acceleration.

A significant improvement in simulation accuracy is seen with the addition of nonlinear component models. The nonlinear quarter car model is assessed at two excitation frequencies, 6.8 and 11.2 Hz. The shock absorber is modelled as a trilinear element and the tyre as a hardening/softening spring with parallel hysteretic damping. The accuracy of the nonlinear simulation is, in part, due to the accuracy with which the trilinear shock absorber model represents the most significant nonlinearity of the shock absorber, namely the static friction. This is illustrated in Figure 9. The trilinear model accounts for both the high damping in the static friction zone and also the lower damping in compression and rebound outside this zone. The different influences of the trilinear and linear models on simulation results are seen at the unsprung mass acceleration peaks in Figure 11. These are regions where shock absorber acceleration is close to its maximum, and shock absorber velocity is a close to zero. The high damping of the trilinear model in this zone causes a visible decrease in shock absorber acceleration. This is in line with the signal pattern observed from measured signals. The linear model cannot account for this phenomenon.

The effect of tyre damping on simulation accuracy was assessed at an excitation frequency of 10.4 Hz. It is shown to have a moderate influence on the simulation accuracy at this frequency. The simulation with tyre damping shows more realistic unsprung mass peak accelerations and as a result lower sprung mass acceleration. The argument put forward by a number of authors is that tyre damping can be neglected in simulations of this type. The results show that although it has an influence on the simulation accuracy, its effect is relatively small when compared with the effect the shock absorber model has on the simulation accuracy. In developing a nonlinear quarter car model, the effectiveness of the shock absorber model should first be examined before focusing on modification of the tyre model to improve simulation accuracy.

Narrowband excitation, in the form of an approximately sinusoidal excitation, is used throughout the experimental and simulation work carried out in this paper. Results show that, for this type of excitation, the nonlinear quarter car model outperforms the linear quarter car model when compared with measured data from the experimental test rig. It is noted that during the isolated shock absorber testing, the shock absorber characteristic shows significant frequency and amplitude dependence, a common observation during shock absorber experimental testing [47,48]. Due to the narrowband nature of the excitation in this investigation, it is possible to assess the accuracy of linear and nonlinear quarter car models at individual frequencies and amplitudes. Under broadband excitation, the frequency and amplitude dependence of the shock absorber may need to be accounted for. Also modes not excited in this investigation may affect simulation accuracy. This is also true for the case of tyre damping; under broadband excitation, all tyre modes are excited and hence the effect of tyre damping, assessed here under narrowband excitation, may be different.

This paper is intended to give an insight into linear quarter car accuracy by highlighting the performance improvement to be had by including nonlinear components in a quarter car simulation subject to narrowband excitation. The results apply to passive suspension components only. The results may vary in the presence of semi-active and active suspension components. The experimental testing is carried out in a controlled laboratory environment using a purpose-built test rig. The test rig cannot replicate certain dynamic behaviour of a vehicle in operation, such as body roll and pitch motions, chassis modes of vibration and handling manoeuvres. To study this topic further, and perform an in-depth investigation into linear quarter car model accuracy, a quarter car experimental test rig capable of broadband excitation or on road full car testing would be required.

6. Conclusions

An experimental test rig featuring a novel force sensor setup was used to test the accuracy of the widely used quarter car experimentally vehicle suspension, model. The force sensor setup allowed the shock absorber force to be measured during operation. This facilitated the development of both linear and trilinear shock absorber models from experimental test results. This approach allowed for optimised linear and trilinear shock absorber models to be developed for individual excitation frequencies. The technique of fitting models at each individual frequency was required due to the nonlinear nature of the shock absorber.

Linear quarter car simulations were carried out with the goal of assessing the accuracy of the linear quarter car model subject to narrowband excitation. The results were compared to measurements from the quarter car experimental test rig with passive shock absorber. The quarter car model was found to give a reasonable approximation of the unsprung mass amplitude in the 1.6 – 24 Hz frequency range for an approximately sinusoidal excitation. It did, however, overpredict the amplitude of the sprung mass acceleration. A nonlinear simulation was developed and compared with the linear simulation and measured results. The nonlinear simulation featured a trilinear shock absorber model and nonlinear tyre with damping. Nonlinear simulation results were examined at two excitation frequencies and were significantly more accurate than linear simulation results in terms of amplitude and signal peak pattern when compared with measured results.

A final investigation examined the effect of tyre damping on the quarter car model results for narrowband excitation at a single frequency. Tyre damping was shown to lower the magnitude of the peaks in the unsprung mass acceleration and was also found to increase the accuracy of the simulation when compared with measured results.

Acknowledgements

This work was funded by the Irish Research Council for Science, Engineering and Technology (IRCSET) under the Embark Initiative.

References

- [1] R.E. Roberson and R. Schwertassek, *Dynamics of Multibody Systems*, Springer-Verlag, Berlin, Germany, 1988.
- [2] G.N. Jazar, R. Alkhatib, and M.F. Golnaraghi, *Root mean square optimization criterion for vibration behaviour of linear quarter car using analytical methods*, Veh. Syst. Dyn. 44 (2006), pp. 477–512.
- [3] C. Kim and P.I. Ro, *Reduced-order modelling and parameter estimation for a quarter-car suspension system*, Proc. Inst. Mech. Eng. D, J. Automob. Eng. 214(8) (2000), pp. 851–864.
- [4] C. Kim, P.I. Ro, and H. Kim, *Effect of the suspension structure on equivalent suspension parameters*, Proc. Inst. Mech. Eng. D, J. Automob. Eng. 213 (1999), pp. 457–470.
- [5] R. Majjad, *Estimation of suspension parameters*, IEEE Conference on Control Applications – Proceedings, Hartford, CT, 1997, pp. 522–527.
- [6] A. Yousefi, A. Akbari, and B. Lohmann, *Low order robust controllers for active vehicle suspensions*, Proceedings of the IEEE International Conference on Control Applications, Munich, Germany, 2007, pp. 693–698.
- [7] R.S. Sharp and D.A. Crolla, *Road vehicle suspension system design – a review*, Veh. Syst. Dyn. 16(3) (1987), pp. 167–192.
- [8] C. Halfmann, O. Nelles, and H. Holzmann, *Modeling and identification of the vehicle suspension characteristics using local linear model trees*, IEEE Conference on Control Applications – Proceedings, Vol. 2, 1999, pp. 1484–1489.
- [9] H. Imine, Y. Delanne, and N.K. M'Sirdi, *Road profile input estimation in vehicle dynamics simulation*, Veh. Syst. Dyn. 44(4) (2006), pp. 285–303.
- [10] H. Kowalczyk, *Damper tuning with the use of a seven post shaker rig*, SAE Technical Paper Series, 2002-01-0804, 2002.
- [11] S. Türkay and H. Akçay, *A study of random vibration characteristics of the quarter-car model*, J. Sound Vib. 282 (2005), pp. 111–124.
- [12] L.F.P. Etman, R.C.N. Vermeulen, J.G.A.M. Van Heck, A.J.G. Schoofs, and D.H. Van Campen, *Design of a stroke dependent damper for the front axle suspension of a truck using multibody system dynamics and numerical optimization*, Veh. Syst. Dyn. 38(2) (2002), pp. 85–101.
- [13] G. Georgiou, G. Verros, and S. Natsiavas, *Multi-objective optimization of quarter-car models with a passive or semi-active suspension system*, Veh. Syst. Dyn. 45(1) (2007), pp. 77–92.
- [14] G. Verros, S. Natsiavas, and C. Papadimitriou, *Design optimization of quarter-car models with passive and semi-active suspensions under random road excitation*, J. Vib. Control 11 (2005), pp. 581–606.
- [15] M.M. Elmadyany and Z.S. Abduljabbar, *Linear quadratic gaussian control of a quarter-car suspension*, Veh. Syst. Dyn. 32(6) (1999), pp. 479–497.
- [16] P. Lugner, H. Pacejka, and M. Plochl, *Recent advances in tyre models and testing procedures*, Veh. Syst. Dyn. 43(6–7) (2005), pp. 413–436.
- [17] A.J.C. Schmitz, *A semi-emperical three-dimensional model of the pneumatic tyre rolling over arbitrary uneven road surfaces*, Ph.D. thesis, Delft University of Technology, 2004.
- [18] P.W.A. Zegelaar, *The dynamic response of tyres to brake torque variations and road unevenesses*, Ph.D. thesis, Delft University of Technology, 1998.
- [19] T.D. Gillespie, S.M. Karamihas, D. Cebon, M.W. Sayers, M.A. Nasim, W. Hansen, and N. Ehsan, *Effects of heavy vehicle characteristics on pavement response and performance*, National Cooperative Highway Research Program Report, 353, 1993, pp. 1–126.
- [20] L.R. Miller, *Tuning passive, semi-active, and fully active suspension systems*, Proceedings of the IEEE Conference on Decision and Control Including The Symposium on Adaptive Processes, 1988, pp. 2047–2053.
- [21] S.P. Wilson, N.K. Harris, and E.J. Obrien, *The use of bayesian statistics to predict patterns of spatial repeatability*, Transp. Res. C, Emerg. Technol. 14(5) (2006), pp. 303–315.
- [22] S. Türkay and H. Akçay, *Effect of tire damping on the ride performance potential of active suspension systems*, Proceedings of the SICE Annual Conference, Tokyo, 113, Japan, 2007, pp. 1209–1216.
- [23] J.A. Levitt and N.G. Zorka, *Influence of tire damping in quarter car active suspension models*, Trans. ASME, J. Dyn. Syst. Meas. Control 113(1) (1991), pp. 134–137.
- [24] A.A. Popov and Z. Geng, *Modelling of vibration damping in pneumatic tyres*, Veh. Syst. Dyn. 43 (2005), pp. 145–155.
- [25] S. Türkay and H. Akçay, *Influence of tire damping on the ride performance potential of quarter-car active suspensions*, Proceedings of the IEEE Conference on Decision and Control, 2008, pp. 4390–4395.
- [26] S. Duym, R. Stiens, and K. Reybrouck, *Evaluation of shock absorber models*, Veh. Sys. Dyn. 27 (1997), pp. 109–127.
- [27] J. Lee and D.J. Thompson, *Dynamic stiffness formulation, free vibration and wave motion of helical springs*, J. Sound Vib. 239(2) (2001), pp. 297–320.

- [28] M. Gobbi, G. Mastinu, and M. Pennati, *Indoor testing of road vehicle suspensions*, Meccanica 43(2) (2008), pp. 173–184.
- [29] C. Paré, *Experimental evaluation of semiactive magneto-rheological suspensions for passenger vehicles*, Master's thesis, Virginia Polytechnic Institute and State University, 1998.
- [30] M. Ahmadian and C.A. Paré, *A quarter-car experimental analysis of alternative semiactive control methods*, J. Intell. Mater. Syst. Struct. 11(8) (2000), pp. 604–612.
- [31] M. Ahmadian, F.D. Goncalves, and C. Sandu, *An experimental analysis of suitability of various semiactive control methods for magneto rheological vehicle suspensions*, Proceedings of SPIE – The International Society for Optical Engineering, volume 5760, San Diego, CA, 2005, pp. 208–216.
- [32] J.D. Langdon, *Design and adaptive control of a lab based tire coupled quarter-car suspension test rig for the accurate re-creation of vehicle response*, Master's thesis, Virginia Polytechnic Institute and State University, 2007.
- [33] J.D. Ziegenmeyer, *Estimation of disturbance inputs to a tire coupled quarter car suspension test rig*, Master's thesis, Virginia Polytechnic Institute and State University, 2007.
- [34] F. Giorgetta, M. Gobbi, and G. Mastinu, *On the testing of vibration performances of road vehicle suspensions*, Exp. Mech. 47(4) (2007), pp. 485–495.
- [35] M. Gobbi, F. Giorgetta, P. Guarneri, G. Rocca, and G. Mastinu, *Experimental study and numerical modelling of the dynamic behaviour of tyre/suspension while running over an obstacle*, American Society of Mechanical Engineers, Design Engineering Division (Publication) DE, Chicago, IL, 2006, pp. 195–204.
- [36] M. Gobbi, P. Guarneri, G. Rocca, and G. Mastinu, *Test rig for characterization of automotive suspension systems*, SAE Technical Paper Series, 2008-01-0692, 2008.
- [37] A.M. Burke and O.A. Olatunbosun, *Static tyre/road interaction modeling*, Meccanica 32(5) (1997), pp. 473–479.
- [38] K.J. Kitching, D.J. Cole, and D. Cebon, *Performance of a semi-active damper for heavy vehicles*, J. Dyn. Syst. Meas. Control 122(3) (2000), pp. 498–506.
- [39] M.W. Sayers and S.M. Karamihas, *Interpretation of road roughness profile data – final report*, Tech. Rep. UMTRI9619, University of Michigan Transportation Research Institute, 1996.
- [40] W. Schiehlen and B. Hu, *Spectral simulation and shock absorber identification*, Int. J. Non-Linear Mech. 38(2) (2002), pp. 161–171.
- [41] D. Kowalski, M.D. Rao, J. Blough, S. Gruenberg, and D. Griffiths, *The effects of different input excitation on the dynamic characterization of an automotive shock absorber*, SAE 01NVC-120, 2001.
- [42] M. Weigel, W. Mack, and A. Riepl, *Nonparametric shock absorber modelling based on standard test data*, Veh. Syst. Dyn. 38(6) (2002), pp. 415–432.
- [43] K. Worden and G.R. Tomlinson, *Nonlinearity in Structural Dynamics, Detection, Identification and Modelling*, Institute of Physics Publishing, Bristol, UK, 2001.
- [44] J.S. Bendat and A.G. Piersol, *Engineering Applications of Correlation and Spectral Analysis*, Wiley-Interscience, New York, 1993.
- [45] R.D. Eyres, A.R. Champneys, and N.A.J. Lieven, *Modelling and dynamic response of a damper with relief valve*, Nonlinear Dyn. 40(2) (2005), pp. 119–147.
- [46] M.D. Rao, S. Gruenberg, H. Torab, and D. Griffiths, *Vibration testing and dynamic modeling of automotive shock absorbers*, Proceedings of SPIE – The International Society for Optical Engineering, Vol. 3989, Newport Beach, CA, 2000, pp. 423–429.
- [47] M. Haroon, D.E. Adams, Y.W. Luk, and A.A. Ferri, *A time and frequency domain approach for identifying nonlinear mechanical system models in the absence of an input measurement*, J. Sound Vib. 283 (2005), pp. 1137–1155.
- [48] K. Worden, D. Hickey, M. Haroon, and D.E. Adams, *Nonlinear system identification of automotive dampers: A time and frequency-domain analysis*, Mech. Syst. Signal Process. 23(1) (2009), pp. 104–126.